9. Hauert, C., De Monte, S., Hofbauer, J. & Sigmund, K. Replicator dynamics for optional public good games. *J. Theor. Biol.* **218,** 187–194 (2002).
10. Sugden, R. *The Economics of Rights, Co–operation and Welfare* (Blackwell, Oxford, UK, 1986).
11. Ostrom, E. *Governing the Commons* (Cambridge Univ. Press, Cambridge, 1999).
12. Gintis, H. *Game Theory Evolving* (Princeton Univ. Press, Princeton, New Jersey, 2000).
13. Berkes, F., Feeny, D., McCay, B. J. & Acheson, J. M. The benefits of the commons. *Nature* **340,** 91–93 (1989).
14. Colman, A. M. *Game Theory and Its Applications in the Social and Biological Sciences* (Butterworth-Heinemann, Oxford, UK, 1995).
15. Boyd, R. & Richerson, P. J. Punishment allows the evolution of cooperation (or anything else) in sizable groups. *Ethol. Sociobiol.* **13,** 171–195 (1992).
16. Gintis, H. Strong reciprocity and human sociality. *J. Theor. Biol.* **206,** 169–179 (2000).
17. Fehr, E. & Gächter, S. Cooperation and punishment in public goods experiments. *Am. Econ. Rev.* **90,** 980–994 (2000).
18. Fehr, E. & Rockenbach, B. Detrimental effects of sanctions on human altruism. *Nature* **422,** 137–140 (2003).
19. Schelling, T. C. Hockey helmets, concealed weapons, and daylight saving—study of binary choices with externalities. *J. Confl. Resolut.* **17,** 381–428 (1973).
20. Dawes, R. M. Social dilemmas. *Annu. Rev. Psychol.* **31,** 169–193 (1980).
21. Boyd, R. & Richerson, P. J. The evolution of reciprocity in sizable groups. *J. Theor. Biol.* **132,** 337–356 (1988).
22. Sober, E. & Wilson, D. S. *Unto Other: The Evolution and Psychology of Unselfish Behavior* (Havard Univ. Press, Cambridge, Massachusetts, 1999).
23. Magurran, A. E. & Pitcher, T. J. Provenance, shoal size and the sociobiology of predator-evasion behaviour in minnow shoals. *Proc. R. Soc. Lond. B* **229,** 439–465 (1987).
24. Michor, F. & Nowak, M. A. Evolution - the good, the bad and the lonely. *Nature* **419,** 677–679 (2002).
25. Ridley, M. *The Origins of Virtue* (Penguin, London, 1996).
26. Axelrod, R. & Hamilton, W. D. The evolution of cooperation. *Science* **211,** 1390–1396 (1981).
27. Nowak, M. A. & Sigmund, K. Evolution of indirect reciprocity by image scoring. *Nature* **393,** 573–577 (1998).
28. Wedekind, C. & Milinski, M. Cooperation through image scoring in humans. *Science* **288,** 850–852 (2000).
29. Bolton, G. E., Katok, E. & Ockenfels, A. What's in a reputation? Indirect reciprocity in an image scoring game. Working paper. (Penn State University, 2001).
30. Seinen, I. & Schram, A. *Social status and group norms: indirect reciprocity in a helping experiment. Discussion paper TI2001-003/1* (Tinbergen Institute, Amsterdam, 2001).

Acknowledgements We thank students at the universities of Bonn, Kiel and Hamburg for participation; T. Bakker, H. Brendelberger, E. Heinz, K.-P. Sauer and M. Zbinden for support; C. Hauert for calculating parameters; and the Max-Planck-Institute of Meteorology for hospitality.

Competing interests statement The authors declare that they have no competing financial interests.

Correspondence and requests for materials should be addressed to M.M. (milinski@mpil-ploen.mpg.de).

Cytosolic pH regulates root water transport during anoxic stress through gating of aquaporins

Colette Tournaire-Roux[1], Moira Sutka[1], Hélène Javot[1], Elisabeth Gout[2], Patricia Gerbeau[1]*, Doan-Trung Luu[1], Richard Bligny[2] & Christophe Maurel[1]

[1]*Biochimie et Physiologie Moléculaire des Plantes, Centre National de la Recherche Scientifique (Unité Mixte de Recherche 5004), Institut National de la Recherche Agronomique, Université Montpellier 2 et Ecole Nationale d'Agronomie, Place Viala, F-34060 Montpellier cedex 1, France*
[2]*Physiologie Cellulaire Végétale, Commissariat à l'Energie Atomique, Rue des Martyrs, F-38054 Grenoble cedex 9, France*

* Present address: Phytobiologie Cellulaire, Université de Bourgogne, BP 47 870, F-21078 Dijon cedex, France

Flooding of soils results in acute oxygen deprivation (anoxia) of plant roots during winter in temperate latitudes, or after irrigation[1], and is a major problem for agriculture. One early response of plants to anoxia and other environmental stresses is down-regulation of water uptake due to inhibition of the water permeability (hydraulic conductivity) of roots (Lp_r)[2–5]. Root water uptake is mediated largely by water channel proteins (aquaporins) of the plasma membrane intrinsic protein (PIP) subgroup[6–8]. These aquaporins may mediate stress-induced inhibition of Lp_r[2,4,9] but the mechanisms involved are unknown. Here we delineate the whole-root and cell bases for inhibition of water uptake by anoxia and link them to cytosol acidosis. We also uncover a molecular mechanism for aquaporin gating by cytosolic pH. Because it is conserved in all PIPs, this mechanism provides a basis for explaining the inhibition of Lp_r by anoxia and possibly other stresses. More generally, our work opens new routes to explore pH-dependent cell signalling processes leading to regulation of water transport in plant tissues or in animal epithelia[10].

The molecular bases of aquaporin gating in plants and animals by phosphorylation[11–13] or other mechanisms[14,15] remain elusive. Certain mammalian aquaporins are regulated by external pH[14–16] when expressed in *Xenopus* oocytes. In plants, the water channel activity of purified plasma membrane vesicles can be blocked by protons[17]. We investigated the relevance of this process for regulation of water uptake by roots in *Arabidopsis*.

Roots detached from plants grown in hydroponics were inserted into a pressure chamber and bathed in a well-aerated standard root bathing solution (RBS) at pH 6.0. Applied pressure (P) induced a flow (J_v) of exuded sap, with a linear J_v to P relationship for P up to 0.5 MPa. The slope reported to root dry weight indicates a mean Lp_r of $61.5 \pm 6.7\ ml\ g^{-1}\ h^{-1}\ MPa^{-1}$ ($\pm$s.e.m.; $n = 4$) (Fig. 1a). Oxygen deprivation was induced in the same roots by N_2 bubbling for 30 min in RBS and resulted in a 42% reduction in Lp_r to $35.6 \pm 7.4\ ml\ g^{-1}\ h^{-1}\ MPa^{-1}$ ($\pm$s.e.m.) (Fig. 1a). Because the J_v curves cross the P axis at similar values close to the origin, measurements of J_v at a high (>0.3 MPa) constant P can be used to monitor relative changes in Lp_r. For instance, the anoxic treatment above induced a 46% reduction in J_v at 0.35 MPa. A similar reduction in J_v by $49.2 \pm 3.7\%$ ($\pm$s.e.m., $n = 5$) was observed on another set of plants. Altogether, these results extend to *Arabidopsis* observations previously made in crop species[3,5]. A fall in cytosolic pH is, besides fluctuations in cytosolic Ca^{2+}, one early cellular response that typically accompanies anoxia[18–20]. This response was investigated in *Arabidopsis* roots using *in vivo* proton-decoupled ^{31}P-nuclear magnetic resonance (NMR) spectroscopy. Spectra (see Supplementary Information 1) revealed three major peaks corresponding to phosphorylcholine (P-Cho), at 3.47 parts per million (p.p.m.), and to cytosolic and vacuolar pools of inorganic phosphate (Pi), at 2.45 and 0.55 p.p.m.—pH values of 7.7 and 5.9, respectively. Within the 10 min after the onset of oxygen deprivation, the peaks of cytosolic Pi and P-Cho shifted upfield to 1.94 p.p.m. and 3.38 p.p.m., respectively, indicating a decrease in cytosolic pH to 7.20–7.25 ($n = 3$).

Inhibitors of cytochrome pathway respiration can be used to mimic oxygen deprivation[4,5]. We found that sodium azide (1 mM NaN_3) and potassium cyanide (0.5 mM KCN) induced a marked inhibition of J_v by $87 \pm 1\%$ (NaN_3; $n = 6$) and $81 \pm 1\%$ (KCN; $n = 7$), with half times ($t_{1/2}$) of 2.6 ± 0.2 min and 4.6 ± 0.1 min, respectively (Fig. 1b). Wash out of NaN_3 and KCN induced a significant reversal of J_v inhibition to $92 \pm 3\%$ ($n = 3$) and $76 \pm 3\%$ ($n = 4$) of initial values, respectively, over a similarly short period of time (NaN_3, $t_{1/2} = 4.6 \pm 0.6$ min; KCN, $t_{1/2} = 3.2 \pm 0.7$ min; Fig. 1b). In parallel NMR experiments the chemical shift of P-Cho indicated that exposure of roots to 1 mM NaN_3 or 0.5 mM KCN resulted in a rapid drop in cytosolic pH to a steady-state value of 6.9–7.0 (NaN_3) or 7.0–7.25 (KCN; $n = 3$) after 10–20 min (Fig. 1c; see also Supplementary Information 1). Wash out of the inhibitors resulted in a complete recovery of initial cytosolic pH values (pH 7.7) in less than 5 min (Fig. 1c).

Loading of root cells with 20 mM propionic acid/potassium propionate (KProp), by substituting at constant pH (pH 6.0) the weak acid for 20 mM KCl in a standard RBS, induced a marked drop in cytosolic pH down to 6.5–6.6 ($n = 3$), with a secondary equilibration to steady-state values in the range of pH 6.7–6.8 (Fig. 2b). A

rapid recovery to initial cytosolic pH values was observed on return to standard RBS (Fig. 2b). Parallel pressure chamber measurements indicated that a similar acid load treatment induced a rapid ($t_{1/2} = 3.7 \pm 0.3$ min; $n = 6$) and significant reduction ($71 \pm 3\%$) in J_v (Fig. 2a). On subsequent transfer into control RBS, a significant recovery from J_v inhibition ($70 \pm 6\%$; $n = 4$) occurred rapidly ($t_{1/2} = 1.8 \pm 0.2$ min), before J_v slowly decreased again and stabilized to a slightly reduced, steady-state value (Fig. 2a). Altogether, kinetic measurements of J_v and cytosolic pH under acid load and respiration blockade conditions establish a strong correlation between cytosolic pH and root water transport capacity. The partially irreversible alterations of Lp_r observed after acid load may result from the large amplitude changes in cytosolic and vacuolar pH values and associated metabolic disturbances. Also, root cells that have the most abundant cytosolic Pi pools and thus contribute to most of the NMR signal may not represent the critical barriers for water transport regulation. This may explain further slight discrepancies between kinetic changes in cytosolic pH and J_v. Furthermore, changing the pH between 5.5 and 8.0 of a RBS had no effect on cytosolic pH and did not noticeably alter Lp_r, indicating that, by

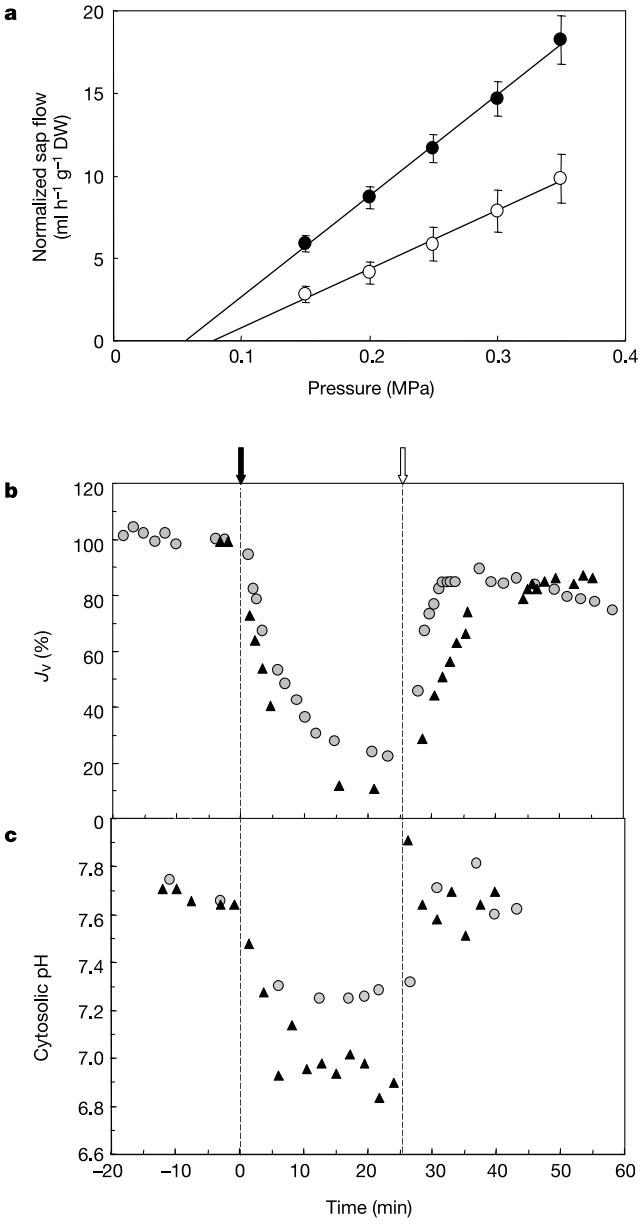

Figure 1 Effects of anoxia and respiratory inhibitors on *Arabidopsis* root water transport and cytosolic pH. **a**, Pressure chamber measurements (±s.e.m.) on individual excised root systems ($n = 4$) bathed in a standard RBS before (normoxic, filled circles) and after (anoxic, open circles) a 30-min bubbling treatment with N_2. J_v was expressed per unit dry weight and plotted as a function of applied pressure. The slope of the regression lines corresponds to the root hydraulic conductivity (Lp_r). **b**, Representative kinetic changes of J_v (% of initial value) induced on two individual excised root systems by exposure to 1 mM NaN_3 (filled triangles) or 0.5 mM KCN (filled circles). Inhibitors were added at $t = 0$ (filled arrow) and removed at $t = 25$ min (open arrow). The applied pressure was kept constant at 0.3 MPa. **c**, Kinetic changes in cytosolic pH in response to exposure to respiratory inhibitors. Same conventions as in **b**.

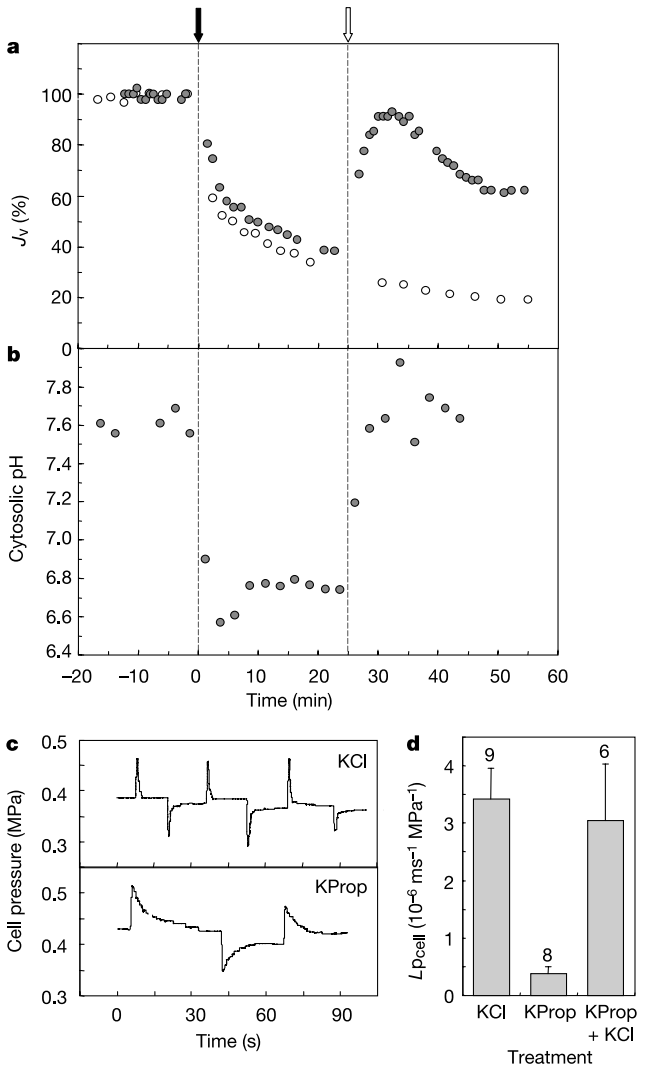

Figure 2 Effects of an acid load on cytosolic pH and water transport in whole roots and cortex cells. **a**, Kinetic changes in J_v induced in response to an acid load with 20 mM propionic acid at pH 6.0. Acid load was applied at $t = 0$ (filled arrow) and maintained (open circles) or reversed (filled circles) at $t = 25$ min (open arrow). **b**, Acid-load-induced changes in cytosolic pH. Same treatment and conventions as in **a**. Cytosolic pH was deduced from the chemical shift of P-Cho determined in 2.5-min acquisition spectra. **c**, Typical time course of root cortex cell pressure relaxation in control (KCl) and acid-loaded (KProp) roots. After measurements of a stationary turgor pressure, exo-osmotic (outward) and endo-osmotic (inward) water movements were triggered by quickly changing the cell pressure using the cell probe, and then hydrostatic relaxations at constant probe volume (meniscus immobilized manually) were recorded. For the individual cells shown, mean water relation parameters were: KCl, $t_{1/2} = 0.50$ s, $Lp_{cell} = 4.16 \times 10^{-6}$ m s^{-1} MPa^{-1}; KProp, $t_{1/2} = 3.98$ s, $Lp_{cell} = 0.44 \times 10^{-6}$ m s^{-1} MPa^{-1}. **d**, Mean Lp_{cell} values for the indicated number of cells from root segments that were pre-treated for 12.5–22.5 min in a KCl or a KProp solution or successively treated for 20 min in KProp and 15–20 min in a KCl solution (KProp + KCl).

contrast to cytosolic pH, extracellular pH does not regulate water transport in *Arabidopsis* roots (data not shown).

Root water transport is mediated through the parallel contribution of cell wall (apoplastic) and cell-to-cell paths[21,22]. The latter includes transport across cellular membranes and/or plasmodesmata and is a likely target for reversible regulation by cytosolic pH. To investigate this, the hydraulic conductivity of root cortex cells (Lp_{cell}) was measured by the cell pressure probe technique[6,23] in conditions similar to those used for measuring J_v and cytosolic pH. Cells of roots bathed in a control saline solution with 20 mM KCl, pH 6.0, displayed typically short hydrostatic equilibration times ($t_{1/2} = 0.66 \pm 0.05$ s; $n = 9$; Fig. 2c) indicative of a high hydraulic conductivity ($Lp_{cell} = 3.43 \pm 0.52 \times 10^{-6}$ m s^{-1} MPa^{-1}; Fig. 2d). In contrast, acid load for 12.5–22.5 min with 20 mM KProp at pH 6.0 resulted in a marked decrease (89%) in Lp_{cell} (Fig. 2d). This decrease was reflected by a greater than tenfold increase in $t_{1/2}$ ($t_{1/2} = 7.29 \pm 1.24$ s; $n = 8$; Fig. 2c) without significant alteration in stationary turgor pressure nor in volumetric elastic modulus (data not shown). Cells from root segments that had been sequentially acid loaded and returned in a control saline solution had a mean Lp_{cell} similar to that of control untreated cells (Fig. 2d). Although cell analysis was only accessible in the cortex[6], the amplitude of acid-load-induced inhibition of Lp_{cell} suggests that blockade of the trans-cellular path can account for most effects observed on whole-root water transport (see Supplementary Information 2).

Because they contribute significantly to Lp_{cell} in roots[6,8], PIP aquaporins may well account for the cytosolic pH-dependent component. The direct effects of extra- and intracellular acidification on the activity of specific PIP isoforms were investigated using heterologous expression in *Xenopus* oocytes. Measurements with a pH-sensitive electrode showed that oocytes maintain physiological cytosolic pH values in the 7.1–7.3 range when exposed to bathing solutions with 50 mM NaCl at pH 7.5 (NaCl 7.5) or pH 6.0 (NaCl 6.0) or with 50 mM sodium acetate at pH 7.5 (NaAc 7.5) (Fig. 3a). In contrast, exposure to 50 mM NaAc at pH 6.0 (NaAc 6.0) induced a marked cytosolic acidification in less than 10 min (cytosolic pH = 5.90 ± 0.06; $n = 8$; Fig. 3a). In parallel osmotic swelling assays, we observed that the osmotic water permeability (P_f) conferred to the oocyte membrane by expression of *Arabidopsis* vacuolar membrane aquaporin TIP1;1 (ref. 24) was insensitive to a 10-min pre-treatment of oocytes by NaCl or NaAc at either pH 6.0 or 7.5 (Fig. 3b). In contrast, the activity of all PIP2 homologues investigated (PIP2;1, PIP2;2, PIP2;3) was markedly (≥85%) and specifically inhibited by a NaAc 6.0 pre-treatment (Fig. 3c). Among several PIP1 isoforms investigated (PIP1;1, PIP1;2, PIP1;3, PIP1;4), only PIP1;2 displayed a significant water transport activity in oocytes, which again was selectively blocked in NaAc 6.0 (Fig. 3d).

The finding that most, if not all, PIPs are specifically blocked by intracellular acidification implies that PIPs have a conserved structural basis for cytosolic pH sensing. Incubation of oocytes expressing PIP2;2 in NaAc solutions with pH between 6.0 and 7.5 (6.0 < cytosolic pH < 6.9) indicated that the apparent pK of proton-dependent PIP inhibition was in the range of pH 6–6.9 (Fig. 4a). This and the sidedness of pH effects suggest that proto-

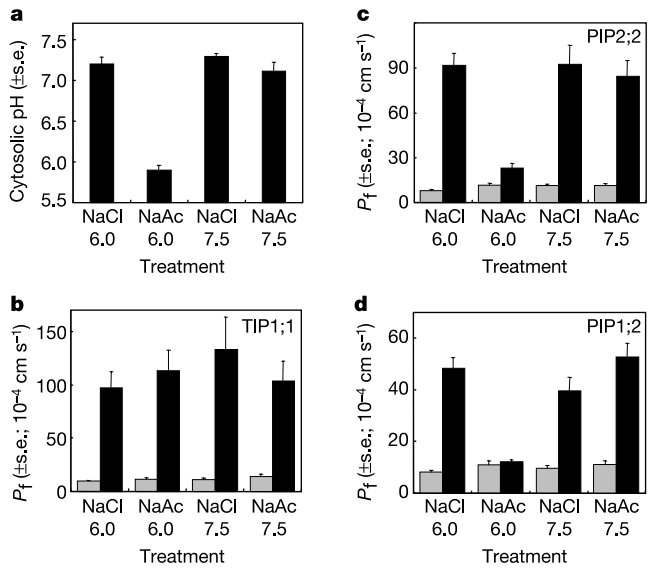

Figure 3 Effects of a stepwise acid load treatment on cytosolic pH and aquaporin water transport activity in *Xenopus* oocytes. **a**, Native oocytes ($n = 7$–8) were pre-treated for 10 min in solutions containing 50 mM NaCl or NaAc at pH 6.0 or pH 7.5, and cytosolic pH was measured in the same solution using a pH-sensitive electrode. **b**–**d**, After pre-treatments as in **a**, P_f of control uninjected (grey bars; $n \geq 11$) or cRNA-injected (black bars; $n \geq 19$; **b**, TIP1;1; **c**, PIP2;2; **d**, PIP1;2) oocytes was measured by a swelling assay in the same solutions but with a fivefold dilution in distilled water. Each panel represents pooled data from three independent batches of oocytes.

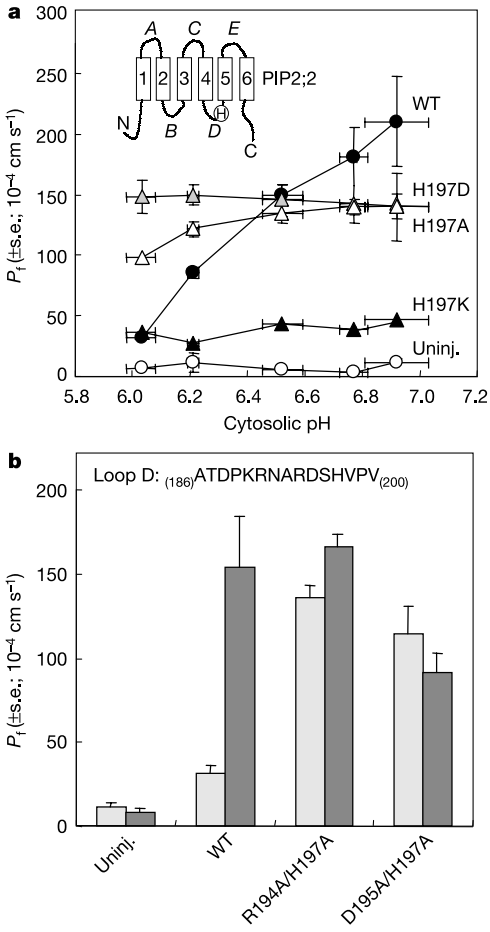

Figure 4 Sensitivity of wild-type (WT) and mutant PIP2;2 to cytosolic acidification. **a**, Control uninjected oocytes (open circles) or oocytes expressing wild-type PIP2;2 (filled circles) or H197D (grey triangles), H197A (white triangles) or H197K (black triangles) mutants were pre-treated for 10 min in NaAc solutions with pH between 6.0 and 7.5. P_f values were measured and are reported as a function of cytosolic pH measured in control oocytes pre-treated in the same conditions. Error bars not shown fall into symbols ($n = 4$–6). The inset shows a schematic view of PIP2;2 topology and the position of H197 (H) in loop D. **b**, Control uninjected oocytes ($n = 9$–10) or oocytes injected with cRNAs ($n \geq 6$) encoding wild-type PIP2;2 or double PIP2;2 mutants R194A/H197A or D195A/H197A were pre-treated in a NaAc 6.0 (light grey bars; cytosolic pH of 6.0) or a NaAc 7.5 (dark grey bars; cytosolic pH of 6.9) solution and their P_f value was measured. The inset shows the sequence of loop D in PIP2;2.

nation of one or more cytoplasmically exposed His residues is involved. Sequence comparison indicated that all 13 *Arabidopsis* PIPs share a highly conserved pattern of five His residues (Supplementary Information 3). Although all PIP1 and certain PIP2 homologues have a few additional His residues at varying positions, PIP2;2 is one PIP isoform that exhibits the minimal five His pattern. Three of these face the cytosol with only two being specific for PIPs: His 197 and His 264, which are localized in intracellular loop D (Fig. 4a, inset) and at the end of the sixth membrane-spanning domain, respectively. In experiments where oocyte cytosolic pH was adjusted to values between 6.0 and 6.9, a PIP2;2 mutant with substitution of His 197 by an Ala residue (H197A) exhibited a much less pronounced blockade by cytosolic acidification (30%) than wild-type PIP2;2 (85%) (Fig. 4a). A H197D mutant carrying a negatively charged Asp at the same position exhibited a constitutively high, pH-insensitive activity. Furthermore, substitution of His 197 by a Lys residue (H197K) conferred a totally pH-insensitive but low apparent activity, in agreement with the assumption that the introduced positive charge may mimic the protonated state of His 197 (Fig. 4a). Altogether, the effects of point mutations and/or charge substitution at position 197 establish His 197 of PIP2;2 as a major site for cytosolic pH sensing. Yet, other titratable residues may account for residual proton sensitivity of H197A channels. A similar mutation at position 264 (H264A), alone or in combination with H197A, had no significant effect on PIP2;2 activity and pH sensitivity (data not shown). Loop D contains a stretch of charged amino acids that also may cooperate with the cytosolic pH-dependent function of His 197 (Fig. 4b, inset). Accordingly, the double mutants R194A/H197A and D195A/H197A displayed a complete insensitivity to cytosolic acidification at pH 6.0 (NaAc 6.0) (Fig. 4b). Single Ala mutants at positions 194 or 195 also showed a markedly reduced inhibition by pH (data not shown). Altogether, these results establish that charged residues in the cytosolic vestibule of the aqueous pore control its conformation and/or conductance and make these responsive to cytosolic protons. Although a His residue is lacking, mammalian aquaporins, including AQP1 and AQP2, also have a stretch of charged amino acids in loop D.

The structural basis described here for cytosolic pH-dependent gating is conserved in all PIPs. This provides a mechanism for coordinate inhibition of plant plasma membrane aquaporins and, as a consequence, for a general block of root water transport, as was observed at the cell and organ levels. Thus, cytosol acidosis was identified as the primary cause for inhibition of Lp_r in anoxic conditions and represents, in addition to changes in cytosolic Ca^{2+} and Rop-dependent H_2O_2 production[20,25], a new signalling mechanism for anoxia. Furthermore, aquaporin mutants with altered sensitivity to cytosolic pH will be instrumental in testing how aquaporin activity in plant roots may be detrimental under anoxic stress, and this may provide new knowledge to improve the flooding tolerance of crops. □

Methods

Plant culture

Arabidopsis thaliana plants (ecotype Wassilewskija) were grown in hydroponic culture as described[6].

Whole-root and cortex cell hydraulic conductivities

The pressure (P)-dependent flow (J_v) of sap exuded by excised roots was measured in a pressure chamber using the device described in ref. 6 and in Supplementary information 2, with a RBS containing 20 mM KCl, 1.25 mM KNO_3, 1.5 mM $Ca(N0_3)_2$, 0.75 mM $MgSO_4$, 0.05 mM KH_2PO_4, 3 mM glucose, 10 mM Mes-KOH, pH 6.0. When indicated, J_v measurements were made in a RBS supplemented with 1 mM NaN_3 or 0.5 mM KCN or in a RBS in which 20 mM propionic acid/potassium propionate (KProp), pH 6.0, was substituted for 20 mM KCl. The dry weight (DW) of individual root systems was determined and hydrostatic hydraulic conductivity (Lp_r) was calculated from the slope of a J_v/DW to P plot derived from steady-state J_v measurements at five P values between 0.15 and 0.35 MPa.

Cell pressure probe measurements were performed as described[6]. Excised root tips (30–50 mm in length) were preincubated in a simplified RBS (KCl) containing 20 mM KCl, 10 mM Mes-KOH, pH 6.0, or in a corresponding acid load solution (KProp: 20 mM K-propionate, 10 mM Mes-KOH, pH 6.0), and the hydraulic conductivity of root cortex cells (Lp_{cell}) located between 2.5–3.5 mm from root apex was measured in the following 12–20 min.

In vivo NMR analyses

^{31}P-NMR spectra of excised roots (approximately 10 g fresh weight) were recorded at 20 °C in an AMX 400 wide bore spectrometer (Bruker) equipped with a 25-mm multinuclear probe tuned at 161.9 MHz, using an experimental arrangement described previously[19]. The acquisition of data used 70-μs pulses (50°) at 0.6-s intervals, and a sweep width of 9.8 kHz. A broadband decoupling at 2.5 W during acquisition and 0.5 W during the delay was applied using the Waltz sequence; the signal was digitized at 4,000 data points zero-filled to 8,000, and processed with a 5-Hz line broadening. Spectra were referenced to methylene diphosphonic acid (pH 8.9) as described[19]. Roots were continuously perfused at a rate of 120 ml min^{-1} with a RBS bubbled with O_2 or N_2 (anoxia) (gas flow of 1 l min^{-1}) in the medium reservoir. This device provides an optimal supply of O_2 in control conditions and allows one to evacuate the CO_2 produced by roots in anoxic conditions.

To assign the resonance of inorganic phosphate and soluble phosphate-containing compounds to specific peaks observed on *in vivo* ^{31}P-NMR spectra, the spectra of perchloric acid extracts prepared from the samples frozen immediately after *in vivo* analyses were compared with the spectra of standard solutions of known compounds[19]. The definitive assignments were made after running a series of spectra obtained by addition of the authentic compounds to the perchloric acid extracts at different pH values. Intracellular pH values were estimated from the chemical shift of the cytosolic and vacuolar Pi pools as previously described[19]. When the peak of cytosolic Pi was too weak to be unambiguously identified, cytosolic pH was evaluated from the chemical shift of the relatively abundant P-Cho (see Supplementary Information 1).

Expression in oocytes, water permeability and cytosolic pH

The complementary DNA of all aquaporins investigated was cloned in a pSP64T-derived expression vector[24]. Aquaporin mutants were generated by oligonucleotide-directed mutagenesis using a recombinant PCR technique[13] or the QuikChange Site-Directed Mutagenesis kit (Stratagene). All the constructs were verified by automated sequencing of the full cDNA. Complementary RNA production, expression in *Xenopus* oocytes and osmotic water permeability (P_f) measurements were performed as previously described[13]. Intracellular pH was measured with respect to a membrane potential electrode using a H^+-selective liquid exchanger microelectrode (hydrogen ionophore II Cocktail A, Fluka) connected to a high impedance amplifier as described[26]. Electrodes had a linear response with a slope ≥52 mV pH $unit^{-1}$.

Received 18 February; accepted 5 June 2003; doi:10.1038/nature01853.

1. Vartapetian, B. B. & Jackson, M. B. Plant adaptations to anaerobic stress. *Ann. Bot.* **79** (Suppl. A), 3–20 (1997).
2. Clarkson, D. T. *et al.* Root hydraulic conductance: diurnal aquaporin expression and the effects of nutrient stress. *J. Exp. Bot.* **51,** 61–70 (2000).
3. Birner, T. P. & Steudle, E. Effects of anaerobic conditions on water and solute relations, and on active transport in roots of maize (*Zea mays* L.). *Planta* **190,** 474–483 (1993).
4. Kamaluddin, M. & Zwiazek, J. J. Metabolic inhibition of root water flow in red-osier dogwood (*Cornus stolonifera*) seedlings. *J. Exp. Bot.* **52,** 739–745 (2001).
5. Zhang, W. H. & Tyerman, S. D. Effect of low O_2 concentration and azide on hydraulic conductivity and osmotic volume of the cortical cells of wheat roots. *Austr. J. Plant Physiol.* **18,** 603–613 (1991).
6. Javot, H. *et al.* Role of a single aquaporin isoform in root water uptake. *Plant Cell* **15,** 509–522 (2003).
7. Martre, P. *et al.* Plasma membrane aquaporins play a significant role during recovery from water deficit. *Plant Physiol.* **130,** 2101–2110 (2002).
8. Siefritz, F., Tyree, M. T., Lovisolo, C., Schubert, A. & Kaldenhoff, R. PIP1 plasma membrane aquaporins in tobacco: from cellular effects to function in plants. *Plant Cell* **14,** 869–876 (2002).
9. Zhang, W. H. & Tyerman, S. D. Inhibition of water channels by $HgCl_2$ in intact wheat root cells. *Plant Physiol.* **120,** 849–857 (1999).
10. Parisi, M. & Bourguet, J. Effects of cellular acidification on ADH-induced intramembrane particle aggregates. *Am. J. Physiol.* **246,** C157–C159 (1984).
11. Han, Z., Wax, M. B. & Patil, R. V. Regulation of Aquaporin-4 water channels by phorbol ester-dependent protein phosphorylation. *J. Biol. Chem.* **273,** 6001–6004 (1998).
12. Johansson, I. *et al.* Water transport activity of the plasma membrane aquaporin PM28A is regulated by phosphorylation. *Plant Cell* **10,** 451–459 (1998).
13. Maurel, C., Kado, R. T., Guern, J. & Chrispeels, M. J. Phosphorylation regulates the water channel activity of the seed-specific aquaporin α-TIP. *EMBO J.* **14,** 3028–3035 (1995).
14. Yasui, M. *et al.* Rapid gating and anion permeability of an intracellular aquaporin. *Nature* **402,** 184–187 (1999).
15. Zeuthen, T. & Klaerke, D. A. Transport of water and glycerol in Aquaporin 3 is gated by H^+. *J. Biol. Chem.* **274,** 21631–21636 (1999).
16. Németh-Cahalan, K. L. & Hall, J. E. pH and calcium regulate the water permeability of Aquaporin 0. *J. Biol. Chem.* **275,** 6777–6782 (2000).
17. Gerbeau, P. *et al.* The water permeability of *Arabidopsis* plasma membrane is regulated by divalent cations and pH. *Plant J.* **30,** 71–81 (2002).
18. Felle, H. H. pH: signal and messenger in plant cells. *Plant Biol.* **3,** 577–591 (2001).
19. Gout, E., Boisson, A.-M., Aubert, S., Douce, R. & Bligny, R. Origin of the cytoplasmic pH changes during anaerobic stress in higher plant cells. Carbon-13 and phosphorous-31 nuclear magnetic resonance studies. *Plant Physiol.* **125,** 912–925 (2001).
20. Subbaiah, C. C., Bush, D. S. & Sachs, M. M. Elevation of cytosolic calcium precedes anoxic gene expression in maize suspension-cultured cells. *Plant Cell* **6,** 1747–1762 (1994).
21. Steudle, E. & Peterson, C. A. How does water get through roots? *J. Exp. Bot.* **49,** 775–788 (1998).
22. Javot, H. & Maurel, C. The role of aquaporins in root water uptake. *Ann. Bot.* **90,** 301–313 (2002).
23. Tomos, A. D. & Leigh, R. A. The pressure probe: a versatile tool in plant cell physiology. *Annu. Rev. Plant Physiol. Plant Mol. Biol.* **50,** 447–472 (1999).
24. Maurel, C., Reizer, J., Schroeder, J. I. & Chrispeels, M. J. The vacuolar membrane protein γ-TIP creates water specific channels in *Xenopus* oocytes. *EMBO J.* **12,** 2241–2247 (1993).

25. Baxter-Burrel, A., Yang, Z., Springer, P. S. & Bailey-Serres, J. RopGAP4-dependent Rop GTPase rheostat control of *Arabidopsis* oxygen deprivation tolerance. *Science* **296,** 2026–2028 (2002).
26. Lacombe, B., Pilot, G., Gaymard, F., Sentenac, H. & Thibaud, J.-B. pH control of the plant outwardly-rectifying potassium channel SKOR. *FEBS Lett.* **466,** 351–354 (2000).

Supplementary Information accompanies the paper on **www.nature.com/nature**.

Acknowledgements We thank H. Höfte, H. Sentenac and C. Vander Willigen for critical reading of the manuscript; N. Declerk for discussions; Y. Boursiac for help with cell pressure probe measurements; and J. B. Thibaud and C. Plassard for assistance in micro-electrode pH measurements. This work was supported in part by the Centre National de la Recherche Scientifique (Action Thématique Incitative sur Programme et Equipe 'Function and regulation of plant aquaporins'). M.S. is on leave from the Laboratorio de Biomembranas, Departamento de Fisiología, Facultad de Medicina, Universidad de Buenos Aires, Argentina.

Competing interests statement The authors declare that they have no competing financial interests.

Correspondence and requests for materials should be addressed to C.M. (maurel@ensam.inra.fr).

ER–phagosome fusion defines an MHC class I cross-presentation compartment in dendritic cells

Pierre Guermonprez[1]*, Loredana Saveanu[2]*, Monique Kleijmeer[3], Jean Davoust[4], Peter van Endert[2] & Sebastian Amigorena[1]

[1]*INSERM U520, Institut Curie, 26 rue d'Ulm, 75005 Paris, France*
[2]*INSERM U580, Institut Necker, 161 rue de Sèvres, 75015 Paris, France*
[3]*Department of Cell Biology, UMC Utrecht, Heidelberglaan 100, 3584 CX Utrecht, The Netherlands*
[4]*CNRS UMR8115, Genethon, 1 bis rue de l'Internationnale, 91002 Cedex 02, Evry, France*

* These authors contributed equally to this work

Induction of cytotoxic T-cell immunity requires the phagocytosis of pathogens, virus-infected or dead tumour cells by dendritic cells[1]. Peptides derived from phagocytosed antigens are then presented to CD8$^+$ T lymphocytes on major histocompatibility complex (MHC) class I molecules, a process called "cross-presentation"[2,3]. After phagocytosis, antigens are exported into the cytosol and degraded by the proteasome[4–6]. The resulting peptides are thought to be translocated into the lumen of the endoplasmic reticulum (ER) by specific transporters associated with antigen presentation (TAP), and loaded onto MHC class I molecules by a complex "loading machinery" (which includes tapasin, calreticulin and Erp57)[7]. Here we show that soon after or during formation, phagosomes fuse with the ER. After antigen export to the cytosol and degradation by the proteasome, peptides are translocated by TAP into the lumen of the same phagosomes, before loading on phagosomal MHC class I molecules. Therefore, cross-presentation in dendritic cells occurs in a specialized, self-sufficient, ER–phagosome mix compartment.

The reasons why phagocytosis itself favours cross-presentation in dendritic cells and macrophages are unclear. To gain further insight into this process, we purified phagosomes from immature dendritic cells. After purification, the enrichment of various phagosomal markers was analysed by western blotting. Early phagocytic markers, such as transferring receptor and phosphoinositide-3-kinase (Pi3Kp85), were detected early after engulfment and rapidly decreased thereafter. Markers of the late endocytic pathway, such as rab7 (Fig. 1a) and Lamp2 (Fig. 1b, left panels) increased over time, indicating phagosome maturation towards phagolysosomes.

In macrophages, phagosomes were recently shown to fuse with the ER during or soon after engulfment[8]. Similarly, we found that several ER resident proteins such as sec61/sec62 and calnexin were detected immediately after phagosome formation in dendritic cells (Fig. 1a and Fig. 1b, right panels). Recruitment of ER residents into phagosomes, however, was restricted to a subset of the ER proteins detected by polyclonal antibodies raised against whole ER membranes (Supplementary Information SD1). The presence of these ER markers in phagosomes decreased as phagosomes matured into phagolysosomes.

To quantify the proportion of phagosomes bearing ER markers, we used flow cytometric (FACS) analysis of phagosomes[9]. After the pulse with latex beads, only 10% of the phagosomes expressed Lamp2, and the proportion of Lamp2-bearing phagosomes increased over time (Fig. 1b, left panel), to reach over 50% after 240 min chase. The distribution of calnexin, in contrast, was homogeneously high in early phagosomes (right panels in Fig. 1b), suggesting that most of the phagosomes had already fused with ER membranes. Consistent with our biochemical analysis and with previous results in macrophages[8], calnexin labelling of phagosomes decreased over time.

ER recruitment to phagosomes was also shown in whole cells, using confocal-laser scanning-microscopy (CLSM). In immature dendritic cells pulsed with fluorescent beads, staining of the phagosomal membrane was observed using both total ER antibodies (not shown) and calnexin antibodies (Fig. 1e), in a wide proportion of early phagosomes. Electronic microscopy analysis of ER distribution by calreticulin staining demonstrates the juxtaposition of ER membranes to the forming phagosomes (phagocytic cups were stabilized by PI3K inhibitors[8]), and strongly suggests direct fusion between the two organelles (Fig. 1c). Direct evidence for ER–phagosome fusion was obtained using a cytochemical EM technique, revealing the activity of the ER enzyme glucose-6-phosphatase (G-6-Pase) on Epon sections[10]. G-6-Pase activity appears as dense precipitates in numerous ER structures throughout the cells, including the nuclear envelope (Fig. 1d). Strikingly, the majority of phagosomes displayed strong G-6-Pase labelling sometimes over the whole of the limiting membrane (Fig. 1d, right panel), other times on part of it (Fig. 1d, left panel). We concluded that in dendritic cells, like in macrophages[8], phagosomes fuse with the ER, soon after or during particle engulfment. ER proteins then progressively disappear as phagosomes mature into phagolysosomes.

Fusion with the ER and the recruitment of ER proteins to phagosomes led us to reconsider the conventional view of cross-presentation. We hypothesized that after antigen export to the cytosol and degradation by the proteasome, peptides could be translocated back into the lumen of the same phagosome by TAP, and loaded onto MHC class I molecules in the phagosomal lumen.

To test this model, we first examined whether ER fusion with phagosomes actually results in recruitment of TAP and of the MHC class I loading machinery. Abundant TAP was detected in early phagosomes and was reduced over time (Fig. 2a, right panel). Flow cytometric analysis of phagosome populations[9] of various ages revealed homogeneous staining of early phagosomes, which also decreased over time (Fig. 2a, left panel). EM analysis of purified phagosomes showed that TAP2 is inserted into the phagosomal membrane surrounding the latex bead (Fig. 2b). The recruitment of TAP to phagosomes was also seen in intact dendritic cells using CLSM (Fig. 2c). In spite of high staining of abundant ER membranes throughout the cells, enrichment in membranes surrounding the beads was evident in most phagosomes.

Together with TAP, tapasin, calreticulin, ERp57 and the heavy chain of MHC class I were all detected in purified early phagosomes by western blotting (Fig. 2d). A clear decrease over time was observed for tapasin and ERp57, whereas MHC class I heavy chain and calreticulin remained stable. Therefore, in the first few